Published online 3 February 2014

Nucleic Acids Research, 2014, Vol. 42, No. 7 ***e58***
doi:10.1093/nar/gku074

Design and application of cotranscriptional non-enzymatic RNA circuits and signal transducers

Sanchita Bhadra and Andrew D. Ellington*

Department of Chemistry and Biochemistry, Institute for Cellular and Molecular Biology, Center for Systems and Synthetic Biology, University of Texas at Austin, Austin, TX 78712, USA

Received October 3, 2013; Revised December 11, 2013; Accepted January 2, 2014

ABSTRACT

Nucleic acid circuits are finding increasing real-life applications in diagnostics and synthetic biology. Although DNA has been the main operator in most nucleic acid circuits, transcriptionally produced RNA circuits could provide powerful alternatives for reagent production and their use in cells. Towards these goals, we have implemented a particular nucleic acid circuit, catalytic hairpin assembly, using RNA for both information storage and processing. Our results demonstrated that the design principles developed for DNA circuits could be readily translated to engineering RNA circuits that operated with similar kinetics and sensitivities of detection. Not only could purified RNA hairpins perform amplification reactions but RNA hairpins transcribed *in vitro* also mediated amplification, even without purification. Moreover, we could read the results of the non-enzymatic amplification reactions using a fluorescent RNA aptamer 'Spinach' that was engineered to undergo sequence-specific conformational changes. These advances were applied to the end-point and real-time detection of the isothermal strand displacement amplification reaction that produces single-stranded DNAs as part of its amplification cycle. We were also able to readily engineer gate structures with RNA similar to those that have previously formed the basis of DNA circuit computations. Taken together, these results validate an entirely new chemistry for the implementation of nucleic acid circuits.

INTRODUCTION

Nucleic acids are versatile molecules that store and process information in living systems. In addition, though, the relatively simple rules for base-pairing interactions have led to the extraordinary blossoming of nucleic acids as molecules that are suitable for nanoscale computation and engineering (1). In the past decade an increasingly complex array of nucleic acid circuits and devices has been engineered both *in vitro* and *in vivo* based on programmed strand displacement (1–9). Short complementary single-stranded domains termed 'toeholds' provide a means of initiating more extensive branch migration reactions. Ultimately, the toehold-mediated non-enzymatic interactions between substrates are driven by the free energy of strand displacement, either via the formation of more net base pairs (enthalpy gain) or via the release of strands from complexes (entropy gain) (4).

Of particular interest is a programmable DNA circuit known as catalytic hairpin assembly (CHA) (10). In CHA two partially complementary DNA hairpins are prevented from reacting with one another by ensconcing the complementary sequences within hairpin structures, effectively leading to kinetic trapping of the reaction (2) (Figure 1a). A short single-stranded oligonucleotide 'catalyst' that can interact with a toehold on one of the hairpins leads to strand displacement and the revelation of sequences that can interact with the other hairpin, the formation of a double-stranded product and the recycling of the catalyst (Figure 1a). Such CHA circuits have recently been developed into sequence-specific signal transduction tools for detection and quantitation of isothermal nucleic acid amplification reactions (11,12).

Because RNA molecules have predictable base-pairing properties similar to DNA and are also capable of hybridization and strand displacement, it should be possible to develop nucleic acid circuits based on RNA and DNA. Although some synthetic *in vitro* transcription circuits have previously been described, these are predominantly hybrid systems in which transcribed RNAs act on DNA promoters (17–20). Limited synthetic circuits involving RNA–RNA hybridization and strand displacement have been applied to transcriptional and translational regulation *in vivo*, but the behavior of these circuits is often unpredictable, possibly because of the potential cross-reactivities that abound within a complex cellular environment (8,9,21). Delebecque *et al.* demonstrated a particularly interesting *in vivo* assembly of rationally

*To whom correspondence should be addressed. Tel: +1 512 232 3424; Fax: +1 512 471 7014; Email: ellingtonlab@gmail.com

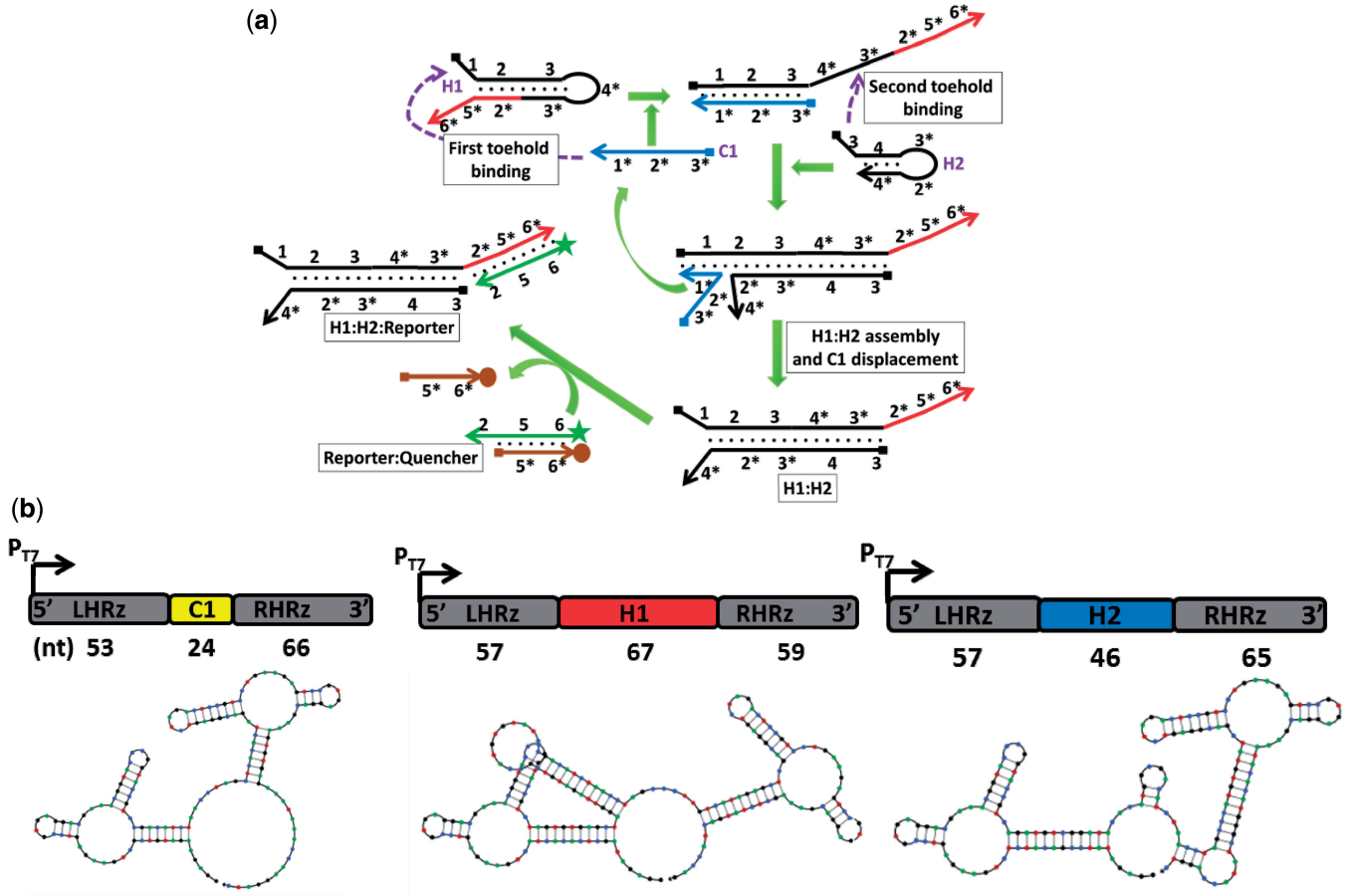

Figure 1. Design of non-enzymatic catalyzed RNA hairpin assembly circuit. (**a**) Schematic of catalyzed nucleic acid hairpin assembly circuit adapted from (2). The circuit composed of hairpins H1 and H2 is turned on in the presence of the input sequence (C1). C1 catalyzes the assembly of H1 and H2 into an H1:H2 duplex and is itself recycled. Circuit output (H1:H2 duplex) is quantitated as increasing fluorescence intensity of a labeled oligonucleotide probe (RepF) on displacement of its complementary quencher oligonucleotide (RepQ) by the H1:H2 duplex. (**b**) Design of T7 RNA polymerase-driven transcription templates for enzymatic synthesis of RNA CHA circuit components with precise 5′- and 3′-ends. Transcription template for each component, H1, H2 and C1, is flanked on both the left (L) and the right (R) sides by hammerhead ribozymes (HRz). The size (in nucleotides) of each component and its ribozyme flanks is indicated under each schematic. Secondary structures of the resulting chimeric RNA at 42°C before ribozyme processing are depicted (green, A; blue, C; black, G; red, U). The RNA structures were generated using NUPACK (13–16).

designed RNA molecules containing dimerization domains, kinetically trapped polymerization domains and aptamer domains into discrete 1D and 2D RNA scaffolds (22). These scaffolds displayed distinct protein-binding sites (aptamers) that were reported to control the spatial organization of a hydrogen-producing pathway in bacteria (22). To widen the scope of such RNA assemblies to different prokaryotic and even eukaryotic cells honing the rules for regulating RNA expression, processing, intra- and intermolecular interactions and transport may prove especially useful.

Therefore, we set out to rationally design a nucleic acid circuit that completely relied on programmed interactions between RNA *in vitro*, rather than on DNA. A RNA CHA circuit was designed based on a well-studied DNA CHA circuit (2). The production of this RNA circuit further required considerable modification for *in vitro* transcription, processing and signal transduction, including engineering the recently described fluorescent RNA aptamer Spinach into a sequence-dependent aptamer beacon that could transduce the circuit output (H1:H2 duplexes) into readable fluorescent signals. However, in operation, the RNA circuits could be directly transcribed from DNA without the need for purification, separation or refolding of the hairpin reactants. Even so, the RNA circuit could detect picomolar concentrations of a catalyst sequence with a median amplification of 87-fold. Turnover rates (v/[C1]) of the RNA CHA circuit were between 0.2 and 1/min, similar to the DNA circuit (2). We believe that such circuits may prove especially useful for the *in situ* generation of substrates for real-time signal transduction of enzymatic isothermal nucleic acid amplification reactions.

These results clearly demonstrate that the base-pairing properties and conformational malleability of RNA can be readily harnessed for executing *in vitro* nucleic acid circuits and also demonstrate the feasibility of RNA I/O computational modules. RNA circuits can be engineered and operated using the same design principles as DNA, but because of the ease of construction of DNA templates

rather than DNA substrates may now render large-scale high-fidelity enzymatic circuit synthesis that is both time and cost-effective. Ultimately, cotranscriptional RNA circuit synthesis *in vitro* may provide a basis for *in vivo* nucleic acid computation and new regulatory paradigms in synthetic biology.

MATERIALS AND METHODS

Reagents, oligonucleotides and transcription templates

Unless otherwise indicated, all molecular-biology-grade chemical reagents were purchased from Sigma-Aldrich (St. Louis, MO, USA). Acrylamide was purchased from Bio-Rad (Hercules, CA, USA), and DFHBI [(Z)-4-(3,5-difluoro-4-hydroxybenzylidene)-1,2-dimethyl-1H-imidazol-5(4H)-one] was a gift from Dr Zhan Zhang (University of Texas at Austin).

All oligonucleotides were obtained from Integrated DNA Technologies (IDT, Coralville, IA, USA). Oligonucleotides were resuspended at 100 μM concentration in Tris:EDTA (TE) (10:0.1) buffer (10 mM Tris–HCl, pH 7.5, 0.1 mM EDTA, pH 8.0) and stored at −20°C. The concentrations of the DNA and RNA suspensions were measured by ultraviolet spectrophotometry using the NanoDrop 1000 spectrophotometer (Thermo Scientific, Wilmington, DE, USA). All transcription templates were built using DNA oligonucleotides obtained from IDT. Short transcription templates (≤60 bp) were initially prepared by annealing two completely complementary oligonucleotides that were mixed in equimolar concentration in TE (10:0.1) buffer containing 50 mM NaCl. The oligonucleotides further underwent denaturation for 5 min at 95°C before being annealed via slow cooling (0.1°C/s) to 25°C; this last step was performed to ensure higher yield and greater structural uniformity. Annealed oligonucleotides were quantitated and used directly for *in vitro* transcription reactions and excess was stored at −20°C. Longer transcription templates were sequentially assembled from sets of shorter overlapping oligonucleotides by oligonucleotide annealing, primer extensions and polymerase chain reaction (PCR) reactions. Site-directed mutagenesis was performed by overlap PCR using mutagenic primers. All DNA enzymatic amplification reactions were performed using high-fidelity Phusion DNA polymerase [New England Biolabs (NEB), Ipswich, MA, USA] or Taq DNA polymerase (NEB), according to the manufacturer's protocols. In some cases, fully assembled transcription templates were subjected to A-tailing by Taq DNA polymerase (NEB). All DNA fragments were either purified using Wizard SV gel and PCR cleanup columns (Promega, Madison, WI, USA) or subjected to agarose gel purification before TOPO-TA cloning into a pCR2.1TOPO plasmid, according to the manufacturer's instructions (Life Technologies, Carlsbad, CA, USA). Cloned plasmids were selected and maintained in an *E. coli* Top10 strain. All transcription templates were verified by sequencing at the Institute of Cellular and Molecular Biology Core DNA Sequencing Facility.

For performing *in vitro* run-off transcription, transcription templates cloned in a pCR2.1-TOPO vector were amplified from sequenced plasmids by PCR using Phusion DNA polymerase. Primers pCR2.1.F and pCR2.1.R specific to the plasmid sequences flanking the insert were used for the amplification of ribozyme-containing transcription templates to ensure uniformity of transcription. For some experiments, RNA CHA circuit components H1B, H2 and C1 were amplified using primers complementary to the exact ends of the cloned inserts (H1B.amp.F:H1B.amp.R, H2.amp.F:H2.amp.R and C1.amp.F:C1.amp.R, respectively) rather than the flanking plasmid. Spinach.ST1 transcription templates were amplified using a primer (pCR2.1F) specific to the flanking plasmid sequence at the 5′-end to maintain uniformity of transcription and a primer (sphT.U.R) specific to the sequence right at the 3′-end of Spinach.ST1 to prevent the incorporation of additional nucleotides. PCR products were analyzed by agarose gel electrophoresis and then purified using the Wizard SV gel and PCR cleanup system, according to the manufacturer's instructions (Promega, Madison, WI, USA).

Circuit design

All RNA structures, circuit designs and interactions were analyzed using NUPACK (13–16). RNA was analyzed at different temperatures using the Serra and Turner, 1995 RNA energy parameters with some Dangle treatment. Free energy comparisons of RNA and DNA sequences were performed with the same parameters; considering that the NUPACK default for RNA sequences is 1 M Na^+ concentration (and zero Mg^{2+} concentration), DNA tests were run with the same concentration.

In vitro transcription

In all, 100 pg to 1000 ng of double-stranded DNA transcription templates was transcribed using 100 U of T7 RNA polymerase (NEB) in 50 μl reactions containing 40 mM Tris–HCl, pH 7.9, 30 mM $MgCl_2$, 10 mM DTT, 2 mM spermidine, 4 mM ribonucleotide (rNTP) mix and 20 U of the recombinant ribonuclease inhibitor RNaseOUT (Life Technologies). Transcription reactions were incubated at 42°C for 1–2 h. After this, transcripts of the circuit components were either (i) used directly for assembly or (ii) subjected to purification before assembly. Transcripts intended for purification were either filtered through Sephadex G25 using the Illustra MicroSpin G-25 columns, according to the manufacturer's instructions (GE Healthcare, Piscataway, NJ, USA), or run through RNA gel purification. Specifically, these latter transcripts were treated with 2 U of DNase I (Epicentre Biotechnologies, Madison, WI, USA) at 37°C for 30 min to degrade the template DNA before RNA gel purification. Any RNA not used directly for circuit assembly was stored for short durations at −20°C, whereas long-term storage was done at −80°C.

Denaturing polyacrylamide gel electrophoresis and RNA gel purification

Ten percent polyacrylamide gels containing 7 M urea were prepared using 40% acrylamide and bis-acrylamide solution, 19:1 (Bio-Rad) in 1× Tris:Borate:EDTA (TBE) buffer (89 mM Tris base, 89 mM boric acid, 2 mM EDTA, pH 8.0) containing 0.04% ammonium persulphate and 0.1% TEMED. An equal volume of 2× denaturing dye (7 M urea, 1× TBE, 0.1% bromophenol blue) was added to the RNA samples. These were incubated at 65°C for 3 min followed by cooling to room temperature before electrophoresis. A single-stranded DNA (ssDNA) ladder prepared by mixing 20, 42, 66 and 99 nt-long oligonucleotides was included as a size marker. The gels were stained for 10 min with SYBR-Gold (Life Technologies) before visualization on the Storm Imager (GE Healthcare). For RNA purification, desired bands were excised from the gel and the RNA was eluted twice into TE (10:1) buffer (10 mM Tris–HCl, pH 7.5, 1 mM EDTA, pH 8.0) and incubated at 70°C and 1000 rpm for 20 min. Acrylamide traces were removed by filtering eluates through Ultrafree-MC centrifugal filter units (EMD Millipore, Billerica, MA, USA) followed by precipitation with 2× volume of 100% ethanol in the presence of both 15 μg GlycoBlue (Life Technologies) and 0.3 M sodium acetate, pH 5.2. RNA pellets were washed once in 70% ethanol. Dried pellets of purified RNA samples were resuspended in 0.1 mM EDTA and stored at −80°C.

Native polyacrylamide gel analysis of RNA circuits

In all, 200 nM each of gel-purified H1 and H2 and 5 nM of gel purified C1 were used to set up 15 μl RNA CHA reactions in 0.2 ml PCR tubes. All RNA components were thawed from −80°C storage and diluted to the desired stock concentrations in 0.1 mM EDTA without refolding. Reactions were assembled at 4°C by mixing circuit components in the indicated combinations in 1× TNaK buffer (20 mM Tris–HCl, pH 7.5, 140 mM NaCl, 5 mM KCl) containing 20 U of RNaseOUT. H1 was added last to the assembled reactions, which were then incubated for 2.5 h in thermocyclers maintained at 42, 52 or 62°C. Following incubation, 10 μl of 50% glycerol was added to each reaction and mixed by pipetting. Fifteen nanograms of C1 alone was similarly prepared as a loading control. All samples were then electrophoresed at room temperature on a native 10% polyacrylamide gel in 1× TBE. A mixture of ssDNA and bromophenol-containing loading dye was used as a size marker. The gels were stained with SYBR®-Gold for 10 min before visualization on the Storm Imager.

Real-time fluorimetric quantitation of RNA CHA circuits assembled from gel-purified RNA

In most experiments, real-time fluorimetric detection of RNA CHA was performed using a RepF:RepQ duplex DNA fluorescence resonance energy transfer (FRET) reporter. This reporter was prepared by annealing the fluorescein (FAM)-labeled fluorescent RepF and quencher RepQ oligonucleotides in a 1:5 molar ratio in 1× TNaK buffer. The oligonucleotides were first denatured for 1 min at 95°C followed by slow cooling at a rate of 0.1°C/s to 25°C to generate annealed duplexes that were then stored in the dark at −20°C. Before circuit assembly, all gel-purified RNA was thawed from −80°C and stored on ice. The refolding of RNA hairpins was deemed unnecessary. The H1 and H2 RNA were diluted to working concentrations in 0.1 mM EDTA. The specific (C1) and non-specific (GQ-C1) catalyst RNA were diluted to working concentrations in 0.1 mM EDTA containing 1 μM oligo dT_{17}. Circuits were assembled on ice in 15 μl reactions by mixing the indicated concentrations of H2 and C1 in 1× TNaK buffer containing 0.5 μM ROX reference dye (glycine conjugate of 5-carboxy-X-rhodamine, succinimidyl ester) (Life Technologies), 20 U of RNaseOUT and 100–400 μM RepF (annealed with 5× excess RepQ). The indicated concentration of H1 RNA was added last to the assembled reactions, in order to initiate circuit assembly; circuits were assembled with 50–400 nM concentrations of H1 and H2 RNA, whereas C1 concentration ranged between 5 pM to 5 nM. Circuit operation was quantitated in 96-well optically clear plates in an ABI 7300 real-time PCR machine (Life Technologies) that was programmed to cycle the circuits through 3 min incubations at 52°C followed by 30 s at 51°C. Fluorescence data were acquired in the FAM and ROX channels. Experiments were performed at least in triplicate and groups of data were statistically compared by single-factor ANOVA followed by Tukey's post hoc analysis.

Real-time fluorimetric quantitation of RNA CHA circuits assembled from cotranscribed RNA

Cotranscriptions were performed using 50 ng each of PCR-amplified H1 and H2 transcription templates; the transcriptions were performed both with different concentrations of C1 and non-specific catalyst GQ-C1 template as well as in the absence of any catalyst template. Transcriptions were mediated by T7 RNA polymerase in 50 μl of reactions that were incubated for 1 h at 42°C. For some experiments, the transcribed RNA was filtered through Sephadex G25 before circuit assembly. For other experiments, the cotranscribed RNA was used directly for RNA CHA quantitation. In most experiments, 2 μl of the cotranscribed RNA components were transferred to 1× TNaK buffer containing 0.5 μM ROX reference dye, 20 U of RNaseOUT and 100–400 μM RepF (annealed with 5× excess RepQ). Reactions were assembled on ice in 15 μl of final volumes and analyzed in 96-well optically clear plates using an ABI 7300 real-time PCR machine that was programmed to cycle the circuits through 3 min incubations at 52°C followed by 30 s at 51°C. Experiments were performed at least in triplicate, and groups of data were statistically compared first by single-factor ANOVA followed by Tukey's post hoc analysis.

RNA CHA-mediated signal transduction of strand displacement amplification

End point RNA CHA-mediated signal transduction of low-temperature SDA

Various concentrations of the ssDNA templates TLTRSDA and 1234LTRSDA were amplified in 25 µl reactions containing 1× NEB Buffer 2 (50 mM NaCl, 10 mM Tris–HCl, 10 mM $MgCl_2$, 1 mM DTT, pH 7.9), 100 nM primer P_{SDA}, 200 nM dNTP, 10 U of Nb.BbvCI (NEB) and 6.25 U of Klenow fragment (3′→5′ exo-) (NEB). The reactions were assembled on ice and then incubated at 37°C for 90 min followed by denaturation for 5 min at 95°C. Samples were then kept at room temperature until end point signal analysis by RNA CHA. The mH1:H2 RNA CHA circuit was cotranscribed using T7 RNA polymerase with 50 ng each of the PCR-amplified hairpin transcription templates. Following 1 h of cotranscription at 42°C, the mH1:H2 RNA CHA circuits were used for end-point strand displacement amplification (SDA) signal transduction either directly (i.e. without purification) or after an initial filtration through Sephadex G25. Five-microliter aliquots of the completed SDA reactions were then incubated in 15 µl of a signal transduction reaction containing 1× TNaK, 0.5 µM ROX reference dye, 20 U if RNaseOUT and 100 nM RepF (annealed with 5× excess of RepQ). Two-microliter aliquots of the cotranscribed mH1:H2 circuits were then added to these reactions for sequence-specific signal transduction of the SDA samples. Control SDA signal transduction reactions included (i) reactions without the SDA templates, (ii) reactions with 2 µl of only the mH1 or H2 RNA and (iii) reactions without any of the RNA CHA components. The fully assembled SDA end point RNA CHA signal transduction reactions were then transferred to 96-well optically clear plates. The FAM and ROX signals were monitored in real-time using an ABI 7300 real-time PCR machine that was programmed to cycle the reactions through 3 min incubations at 52°C followed by 30 s at 51°C.

Real-time RNA CHA-mediated signal transduction of high-temperature SDA

Various concentrations of the ssDNA template 1234HTRSDA were amplified in 20 µl of reactions containing 1× NEB Buffer 2 (50 mM NaCl, 10 mM Tris–HCl, 10 mM $MgCl_2$, 1 mM DTT, pH 7.9), 100 nM primer P_{SDA}, 200 nM dNTP, 10 U of Nb.BsrDI (NEB) and 8 U of *Bst* 2.0 (NEB). For fluorescent quantitation, 0.625 µM ROX reference dye and 75 nM RepF (annealed with 5× excess of RepQ) were included in the reactions. The mH1:H2 RNA CHA circuit was cotranscribed using T7 RNA polymerase from 50 ng each of the PCR-amplified hairpin transcription templates. Following 1 h of cotranscription at 42°C, the mH1:H2 RNA CHA circuits were used for SDA signal transduction either directly (i.e. without purification) or after an initial filtration through Sephadex G25. Two-microliter aliquots of the mH1:H2 circuits were added to the SDA reactions on ice. Control SDA reactions included (i) reactions without the 1234HTRSDA template, (ii) reactions with 2 µl of only the mH1 or H2 RNA and (iii) reactions without any of the RNA CHA components. The fully assembled SDA reactions with real-time RNA CHA were then transferred to 96-well optically clear plates. The FAM and ROX signals were monitored in real-time using an ABI 7300 real-time PCR machine programmed to cycle the reactions through 3 min incubations at 55°C followed by 30 s at 54°C.

Real-time quantitation of RNA CHA with sequence-dependent fluorescent RNA aptamer beacon

Use of Spinach.ST1 RNA aptamer beacon as a sequence-specific signal transducer of RNA CHA

H1B, H2, C1, C2 and Spinach.ST1 RNA were transcribed separately by T7 RNA polymerase using 500 ng of double-stranded transcription templates. Transcription templates for H1B, H2 and C1 were amplified using primers complementary to the exact ends of the cloned inserts (H1B.amp.F:H1B.amp.R, H2.amp.F:H2.amp.R and C1.amp.F:C1.amp.R, respectively) rather than the flanking plasmid. Spinach.ST1 transcription templates were amplified using a primer (pCR2.1.F) specific to the flanking plasmid sequence at the 5′-end and a primer (sphT.U.R) specific to the sequence right at the 3′-end of Spinach.ST1. Transcriptions were performed for 2 h at 42°C followed by filtration of the transcripts through Sephadex G25. RNA CHA reactions with Spinach.ST1 signal transduction were then performed in 15 µl reactions containing 1× TNaK buffer, 20 U of RNaseOUT and 70 µM DFHBI. Three-microliter transcription aliquots of each RNA circuit component—including the hairpins H1B and H2, catalysts C1 and C2 and reporter Spinach.ST1—were added to the CHA reactions as indicated. When C1 and C2 were both added at the same time to RNA CHA reactions, 1.5 µl of each input was included in the reactions. The reactions were transferred to 384-well flat-bottomed black plates and Spinach.ST1 fluorescence was measured in a TECAN Safire plate reader (TECAN, Switzerland) maintained at 37°C.

Comparison of Spinach.ST1 and DNA FRET reporter duplex for gel-purified RNA CHA quantitation

Gel-purified RNA components were used for direct comparison of the efficiency of the two types of fluorescent nucleic acid reporters. The FAM-labeled fluorescent DNA reporter H1B.F was annealed with the quencher oligonucleotide H1B.Q at a 1:2 molar ratio in 1× TNaK buffer. The oligonucleotides were denatured for 1 min at 95°C and then annealed by slow cooling at a rate of 0.1°C/s to 25°C. The RNA components H1B, H2, C1 and Spinach.ST1 were transcribed by T7 RNA polymerase from 1 µg each of PCR-generated transcription templates and purified from denaturing polyacrylamide gels. Stored RNA components were thawed from −80°C and diluted to the desired working concentrations in 0.1 mM EDTA. RNA CHA circuits were assembled from 1 µM each of H1B and H2 RNA in 15 µl reactions containing 1× TNaK buffer and 20 U of RNaseOUT. One set of reactions was quantitated by adding 1 µM H1B.F (annealed with 2× excess of H1B.Q), whereas a second

set was quantitated by adding 1 μM Spinach.ST1 RNA along with 70 μM DFHBI. Background hairpin assembly was measured in the absence of C1 RNA, whereas the efficiency of catalyzed reactions was quantitated by adding different concentrations (between 10–100 nM) of C1 RNA. Reactions were transferred to 384-well flat-bottomed black plates and multilabel fluorescence was captured using a TECAN Safire plate reader maintained at 37°C.

RESULTS AND DISCUSSION

Designing an RNA-based CHA circuit

Although there have been numerous non-enzymatic DNA circuits that have been designed for a variety of algorithms, including amplification, neural networks and even taking square roots, there have been few RNA circuits that have been examined (1–7). In principle, RNA circuits should work much the same way as DNA circuits, as in both instances their execution will be dependent on hybridization and strand exchange. However, the energetics of RNA circuits should be decidedly different than those of a corresponding DNA circuit, as RNA–RNA interactions are much more stable than DNA–DNA interactions (23). To determine how to best design RNA circuits, we initially started with the well-known CHA reaction (2,10) in which two short hairpin species form a double-stranded product only in the presence of a single-stranded catalyst that can bind to a toehold and initiate strand exchange (Figure 1a).

Although it may be possible to chemically synthesize RNA-based circuits in the same manner as DNA-based circuits, the chemical synthesis of RNA is more complex, more expensive and more fraught with error than is the chemical synthesis of DNA. We have recently found that the imperfections present in chemically synthesized substrates in nucleic acid circuits are a persistent source of noise during their execution (24). Therefore, we chose to enzymatically transcribe the substrates for RNA circuits, a procedure that may also provide new options for the design and execution of nucleic acid circuitry in general.

We initially chose to generate an RNA CHA reaction based on DNA CHA reactions that had previously yielded efficient amplification of a single-stranded sequence signal (2). We hypothesized that the RNA CHA circuit would operate optimally under conditions in which the RNA hairpin-free energies were predicted to be similar to that of their DNA counterparts in the parent DNA CHA circuit. A similar hypothesis has recently led us to design thermostable DNA circuits that can be used for the real-time detection of isothermal amplification reactions (12). Thus, instead of redesigning the sequences of the circuit we merely converted the DNA sequence to an RNA sequence (with minor sequence changes to allow hammerhead ribozyme cleavage at the 3′-end of circuit components) and predicted a new thermal optimum.

However, to generate RNA circuit that could be enzymatically transcribed, several design issues had to first be addressed. First, because T7 RNA polymerase is most efficient with a prescribed initiation sequence (25,26), either the hairpin substrates had to be designed around a relatively limited set of sequences, or some means of removing the 5′ termini of a hairpin substrate had to be explored. Similarly, the 3′ ends of RNA transcripts are frequently heterogeneous, with so-called N + 1, non-templated additions of adenosine occurring (25,27), meaning it would be desirable to make the ends flush via some processing mechanism. To maximize design possibilities and ensure homogeneity in the RNA termini, we flanked each RNA substrate with hammerhead ribozymes (Figure 1b), similar to constructs that are frequently used for the preparation of RNA molecules for crystallography (28,29). Additionally, with this design, short transcripts that would result from the abortive cycling of T7 RNA polymerase (25,30) should only contain ribozyme-derived sequences and not domains from the CHA components that could potentially poison the CHA reaction or increase noise. Nascent transcripts undergo cotranscriptional ribozyme self-cleavage to release circuit components with exact 5′- and 3′-ends. The correct-sized substrates can be separated from the processed ribozyme flanks via denaturing polyacrylamide gel electrophoresis (Figure 2a).

When the gel-purified hairpins were mixed together, little reaction was observed, as determined by native polyacrylamide gel electrophoresis (Figure 2b). However, in the presence of the catalyst (C1) RNA input, a CHA reaction and the formation of a double-stranded RNA product was observed at 42 and 62°C, with maximal duplex formation occurring at 52°C. Our *in silico* analyses had predicted 52°C to be the optimal operating temperature for the RNA CHA circuit. At this temperature, the free energies of the RNA circuit components should be most closely matched with the functional parental DNA CHA circuit (Supplementary Table S2). At lower temperatures, the RNA H1 and H2 hairpins were predicted to be too stable, and this led to a reduced accumulation of assembled H1:H2 duplexes (Figure 2b). At higher temperatures, the hairpins were unstable and background H1:H2 duplex assembly in the absence of catalyst increased (Figure 2b). These results confirm that the design principles previously developed for optimizing performance with respect to temperature can also be used to optimize performance with respect to chemistry (the difference between DNA and RNA). In short, the free energy of base pairing is the fundamental parameter for designing functional circuits. A similar set of considerations has led Zhang *et al.* to rules for optimizing toehold lengths for triggering strand exchange (31).

Characterization of RNA CHA circuit kinetics

For real-time quantitative analysis of catalyzed H1:H2 assembly, we used a previously described DNA FRET probe (RepF:RepQ) that was prepared by annealing a 5′-FAM-labeled strand (RepF) to an oligonucleotide that had been 3′-end labeled with the Iowa Black FQ quencher (RepQ) (Figure 1a and Supplementary Table S1). Assembly of the H1:H2 duplex exposes domain 2* that is otherwise sequestered within the stem of free H1.

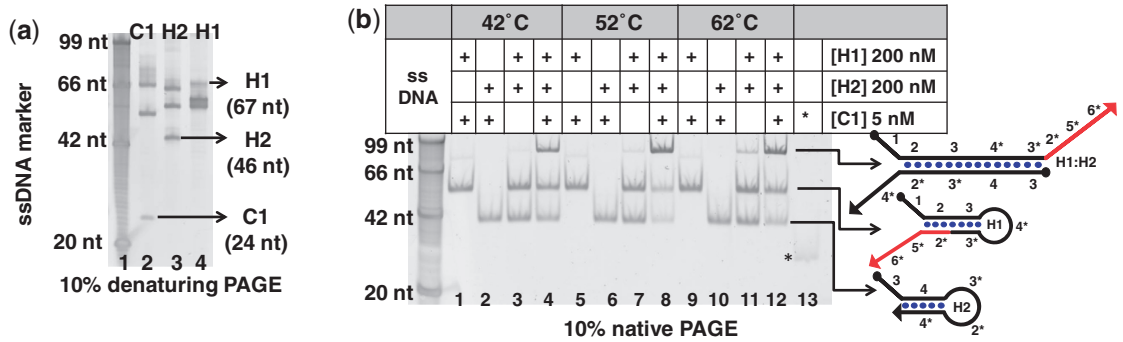

Figure 2. Synthesis and execution of RNA CHA circuit. (**a**) LHRz and RHRz-mediated cotranscriptional RNA cleavage releases the internal circuit components H1, H2 and C1. Fifty nanograms of PCR-generated transcription templates for H1, H2 and C1 was transcribed in 50 µl of reactions by T7 RNA polymerase for 2 h at 42°C. Two microliters of the resulting transcripts was analyzed by electrophoresis on a 10% denaturing polyacrylamide gel. Single-stranded DNA oligonucleotides were used as size markers. (**b**) RNA hairpins undergo catalyzed assembly into RNA duplexes. Gel-purified RNA catalyst C1 and the hairpins H1 and H2 were combined as indicated and incubated in 1× TNaK buffer containing 20 U of RNaseOUT for 150 min at 42°C (lanes 1–4), 52°C (lanes 5–8) or 62°C (lanes 9–12). The reactions were then analyzed on a 10% native polyacrylamide gel. Fifteen nanograms of C1 RNA was included in lane 13 as a control. Single-stranded DNA oligonucleotides were used as size markers.

This domain then acts as a toehold to initiate displacement of the RepQ strand from the RepF:RepQ duplex, ultimately resulting in increased RepF fluorescence. Real-time fluorescence quantification during RNA CHA circuit operation revealed that 5 nM C1 RNA could catalyze rapid accumulation of H1:H2 RNA duplexes at 52°C with reactions approaching completion by 2 h (Figure 3a). The RNA circuit consistently detected picomolar concentrations of the catalyst sequence with a median amplification of 87-fold, similar to that previously observed for the DNA CHA counterpart (2).

The kinetics of catalyzed and uncatalyzed RNA CHA were measured using varying concentrations of gel-purified substrates H1 and H2 in the presence or absence of 2.5 nM gel-purified C1 (Figure 3b and c). Depending on the concentration of the substrates H1 and H2, catalyzed CHA proceeded from 20- to 237-fold faster initial rates when compared with uncatalyzed reactions (Table 1). For any given H2 concentration, the initial catalyzed reaction rate increased with increasing H1 concentration. On the other hand, at any given H1 concentration, the initial rate increased with increasing H2 concentration only until the concentrations of H1 and H2 were equivalent. Excess H2 generally resulted in reduced catalytic rates, possibly because uncatalyzed background hybridization between H1 and H2 removed H1 from the cascade. The strong dependence of the catalytic rate on H1 concentration suggests that the H1:C1 interaction is a rate-limiting step for this circuit. With H1 and H2 concentrations ranging from 50 to 300 nM and 100 to 400 nM, respectively, turnover rates (ν/[C1]) of the RNA CHA circuit were measured to be between 0.2 to 1/min (Figure 3b). This implies that the RNA circuit can be operated to produce 12–60 product units (H1:H2 duplex) per molecule of C1 per hour. This range is similar to that previously achieved with a DNA CHA circuit (2).

Cotranscriptional synthesis of a RNA CHA circuit

We hypothesized that the ribozyme end-processed RNA components H1 and H2 might fold during transcription to create kinetic traps, without the need for additional purification. This hypothesis was based in part on an understanding of the fact that RNA folds sequentially and locally during transcription (32). In keeping with this hypothesis, the cotranscriptional self-cleavage of both the flanking hammerhead ribozymes in the H1, H2 and C1 RNAs (Figure 2a) suggested that proper ribozyme structures were sequentially formed during *in vitro* transcription.

To test our hypothesis, 50 ng of PCR-generated transcription templates of H1 and H2 were cotranscribed in 50 µl reactions in the absence or presence of varying amounts of a C1 transcription template. Following 1 h transcription at 42°C, the reactions and all transcribed species were filtered through Sephadex G25. The FRET probe RepF:RepQ was added to an aliquot of the eluate to monitor circuit output (H1:H2 duplex). The RNA CHA reaction was then carried out at 52°C in 1× TNaK buffer (Figure 4a).

We observed that cotranscribed H1 and H2 showed some reaction in the absence of a catalyst but could undergo much more robust amplification in the presence of cotranscribed catalyst. As controls, transcription reactions lacking T7 RNA polymerase failed to synthesize the circuit and did not activate the reporter, whereas cotranscription of non-specific catalyst sequences also failed to catalyze RNA CHA (Supplementary Figure S1).

Uncatalyzed H1:H2 duplex assembly was unacceptably high in cotranscribed circuits and resulted in end-point signal-to-noise ratios of only between 1 and 1.6. We hypothesized that separating nucleation of toehold interactions from propagation of these interactions might be a way to disrupt uncatalyzed noise resulting from the random breathing or opening of hairpins. The distal ends of the hairpin stems were predicted to be least stable such that the first few bases in H2 domain 4 and H1 domain 2 might be transiently single-stranded due to RNA structural breathing (Figure 1a). Therefore, these bases might function as a weak toehold that led to unintended non-catalyzed base pairing with the already single-stranded loop domains of H1 (domain 4*) and H2

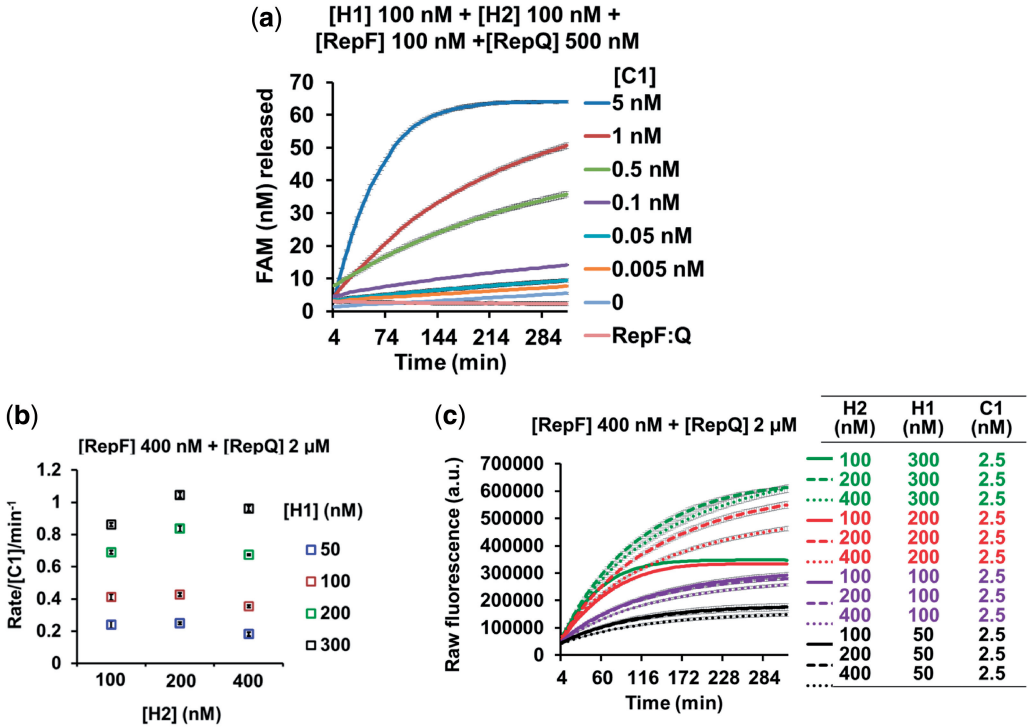

Figure 3. Kinetics and sensitivity of purified RNA CHA circuit. (**a**) Fold amplification and sensitivity of gel-purified RNA CHA circuit. The RNA CHA circuit can detect pure C1 to picomolar concentration with ~87-fold amplification of 0.1 nM C1 within 315 min at 52°C. Circuit output measured as concentration of RepF released from RepF:RepQ duplex was extrapolated from a standard curve of free RepF. (**b**) Initial rate of C1-catalyzed H1:H2 hybridization was measured by incubating varying concentrations of gel-purified H1 and H2 with 2.5 nM pure C1 RNA diluted in 1 μM oligo dT_{17}. Circuits were executed in 1× TNaK buffer containing 20 U of RNaseOUT, 0.5 μM ROX reference dye and 400 nM RepF annealed with 5× excess (2 μM) RepQ at 52°C for 315 min. Initial rates were calculated from circuit output measurements made during the initial 3–20 min of circuit operation. Average data from three separate experiments are represented. H1 concentration has a greater impact on the initial rate suggesting that the first step of the circuit (C1-triggered unfolding of H1) is a rate limiting step. (**c**) Effect of H1 and H2 concentrations on the kinetics of RNA CHA circuit. Average raw fluorescence data from triplicate experiments are plotted. Circuit output is maximal when operated with near equal concentrations of H1 and H2. Increasing H2 concentration above that of H1 generally decreased the initial reaction rate and resulted in reduced circuit output.

Table 1. Initial rates of catalyzed and uncatalyzed RNA CHA[a]

[H2] nM	[H1] nM	Average initial rate/min ± SD	
		[C1] = 2.5 nM	[C1] = 0
100	300	2.15 ± 0.04	0.03 ± 0.02
100	200	1.72 ± 0.05	0.03 ± 0.02
100	100	1.02 ± 0.08	0.01 ± 0.02
100	50	0.6 ± 0.09	−0.004 ± 0.003
200	300	2.61 ± 0.07	0.09 ± 0.01
200	200	2.08 ± 0.08	0.06 ± 0.02
200	100	1.07 ± 0.04	0.02 ± 0.01
200	50	0.62 ± 0.04	0.002 ± 0.002
400	300	2.40 ± 0.08	0.12 ± 0.005
400	200	1.68 ± 0.02	0.07 ± 0.02
400	100	0.88 ± 0.03	0.04 ± 0.002
400	50	0.45 ± 0.05	0.007 ± 0.002

[a]RNA CHA circuits were assembled using gel-purified RNA.

(domain 2*) and in turn to H1:H2 assembly (Supplementary Figure S2). To test this hypothesis, we generated mutant H1 that had a single-stranded loop domain 4* that contained either a two-base (mH1) or one-base (mAH1 and mGH1) mismatch with stem domain 4 of H2 (Figure 4b). The mutant hairpins were designed so as to achieve the strongest mismatches while keeping the domain GC content unaltered. Similarly, a mutant H2 hairpin (m2H2) was designed whose single-stranded loop domain 2* contained a two-base mismatch with the stem domain 2 of H1 (Figure 4c).

We first compared the activities of mutated hairpins in CHA reactions that used gel-purified RNA reactants and catalysts (Supplementary Figures S3 and S4). The catalytic rates of CHA circuits mH1:H2, mAH1:H2 and mGH1:H2 were not significantly different from that of the wild-type H1:H2 circuit (Supplementary Figure S3a and c). However, the non-catalyzed background rate of RNA duplex assembly was significantly reduced for mH1-, mAH1- and mGH1-containing circuits. The two-base mismatch-containing mH1 showed the most reduction (7-fold) in non-catalyzed hairpin assembly, whereas ~3-fold reduction in background was achieved with both mAH1 and mGH1 (Supplementary Figure S3b and d). The H1:m2H2 circuit also demonstrated a significant 7-fold reduction in non-catalyzed assembly of hairpin duplexes (Supplementary Figure S4). These results generally demonstrate that impairing the formation of transient toeholds at the ends of H1 and H2 stems

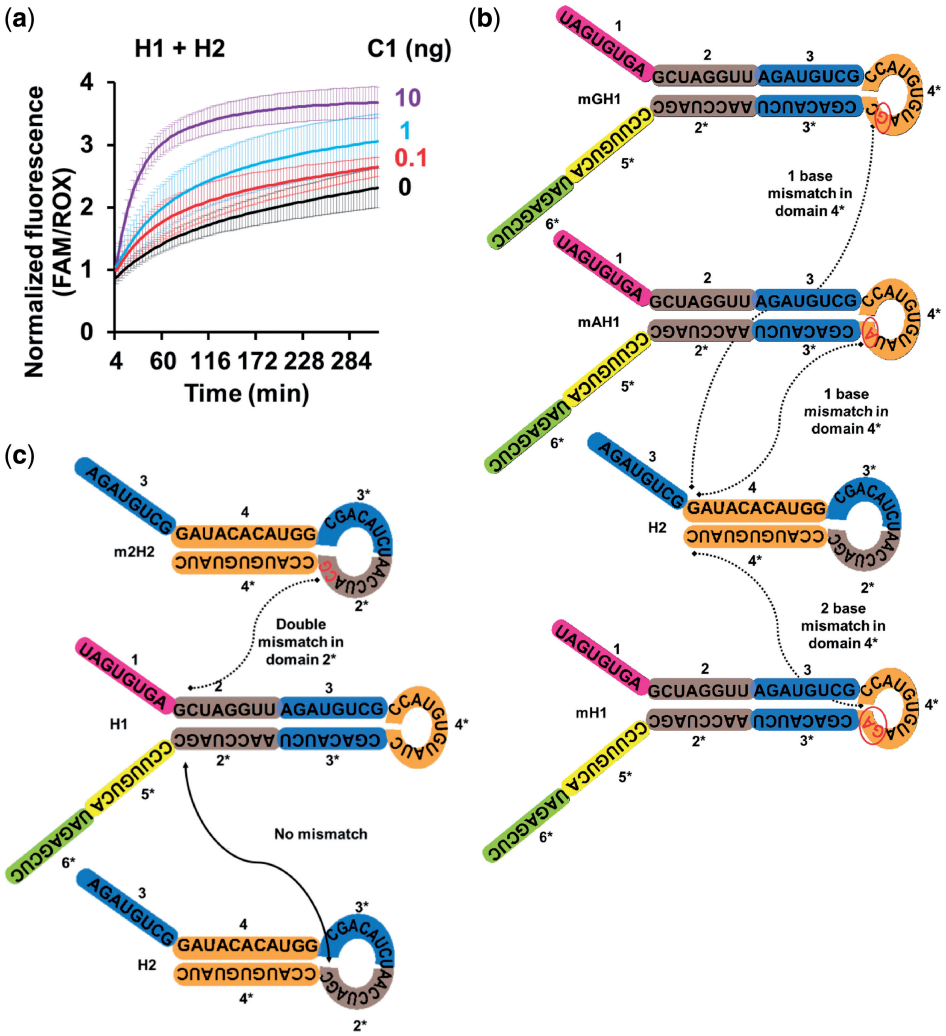

Figure 4. Cotranscriptional RNA CHA and circuit design optimization for cotranscription. (**a**) Cotranscribed RNA circuit components undergo catalyzed hairpin assembly without requiring gel purification of individual reactants. Fifty nanograms each of H1 and H2 transcription templates, along with titrating amounts of C1 transcription template, was cotranscribed for 1 h at 42°C using T7 RNA polymerase followed by passage through Illustra MicroSpin Sephadex G25 columns. Transcription templates were amplified from cloned inserts using primers pCR2.1.F and pCR2.1.R specific to plasmid sequences flanking the inserts. Two microliter aliquots of the cotranscribed RNA mixtures were then incubated in 15 µl of volume with 400 nM RepF annealed with 5× excess (2 µM) RepQ fluorescent DNA reporter duplex in 1× TNaK buffer containing 20 U of RNaseOUT and 0.5 µM ROX reference dye to quantitate formation of H1:H2 RNA duplexes at 52°C. Average data from triplicate experiments are represented. (**b** and **c**) Schematic depicting sequences of RNA hairpins H1 and H2 with one- or two-base engineered mismatches. Mismatched H1 (mH1) presents a two-base mismatch between its domain 4* and domain 4 of H2. The hairpins mAH1 and mGH1 each contain a single mismatched base between their domain 4* and the domain 4 of H2. The mutated H2 hairpin m2H2 presents two mismatched bases between its domain 2* and the H1 domain 2.

significantly reduces uncatalyzed duplex assembly while still maintaining CHA rates similar to those achieved with the original perfectly paired H1 and H2 substrates.

We also sought to determine how mismatched hairpins impacted signal-to-noise ratio under cotranscription conditions. Fifty nanograms of the various hairpins 1 and 2 was cotranscribed with or without 10 ng of the C1 transcription template in 50 µl of reactions. The mH1:H2 and H1:m2H2 CHA circuits operated with statistically similar initial rates of catalyzed hairpin assembly compared with the H1:H2 circuit, and the initial rate of uncatalyzed hairpin assembly for the H1:m2H2 circuit under cotranscription conditions was also similar to that observed with the H1:H2 circuit. However, we observed a statistically significant from 13- to 15-fold reduction in the initial rate of background hairpin assembly in the mH1:H2 circuit compared with both the H1:H2 and H1:m2H2 circuits (Supplementary Figure S5). Cotranscriptionally generated H1:H2 and mH1:H2 RNA CHA circuits remained fully functional even without purification through Sephadex G25, with the best signal-to-noise ratios again being observed with the mH1:H2 circuits (Figure 5a).

Based on these initial results, performance of the mH1:H2 circuit was compared in greater detail with the H1:H2 circuit using varying catalyst concentrations with both gel-purified RNA and cotranscribed circuits. Under most conditions tested, the mH1:H2 and H1:H2 circuits showed comparable catalytic rates, whereas the background hairpin assembly remained minimal in the

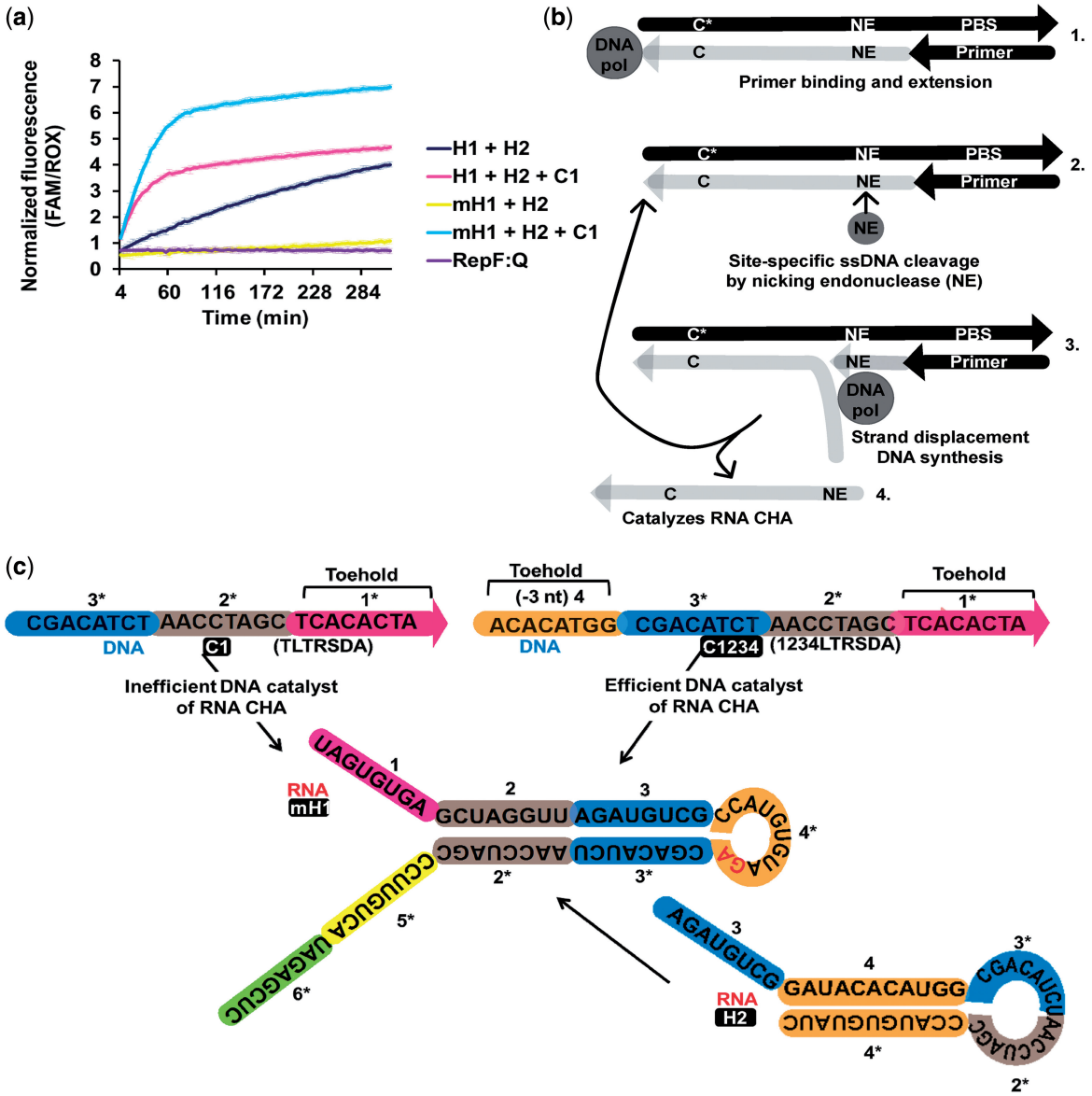

Figure 5. Operation of cotranscriptionally generated RNA CHA circuits without any downstream purification and design optimization for detection of DNA target. (**a**) Fifty nanograms each of the indicated pairs of hairpin 1 and 2 transcription templates was cotranscribed with or without 10 ng of C1 transcription template for 1 h at 42°C using T7 RNA polymerase. Following transcription, 2 µl of the reaction mix was directly incubated in 1× TNaK buffer containing 20 U of RNaseOUT and 0.5 µM ROX reference dye along with 400 nM RepF (annealed with 5× excess RepQ) fluorescent DNA reporter duplex for quantitating RNA CHA in real-time at 52°C. (**b**) Schematic depicting SDA of DNA. The single-stranded template DNA (black arrow) consists of a sequence (C*) complementary to the RNA CHA catalyst followed by the nicking enzyme recognition sequence (NE) that is present on the non-cleaved DNA strand and a primer binding site. Following primer binding (step 1), the DNA polymerase synthesizes the complementary strand that now completes the duplex NE site and contains the RNA CHA catalyst sequence (C). Nicking enzyme then binds the duplex NE site (step 2) and cleaves the newly synthesized strand at the NE site. The new 3′-OH group generated at the nick site is then extended by the DNA polymerase (step 3) while displacing the previously synthesized strand. The displaced ssDNA amplicon can then catalyze RNA CHA. (**c**) Schematic of DNA target sequence design for catalysis of RNA CHA. Single toehold (domain 1*) DNA target C1 (generated by SDA from the template TLTRSDA) with the same domain architecture as the RNA C1 is an inefficient catalyst of RNA CHA. Extended DNA target C1234 (generated by SDA from the template 1234LTRSDA) presenting two toeholds for RNA H1 successfully catalyzes RNA CHA.

mH1:H2 circuit (Supplementary Figure S6). With gel-purified H1:H2 and mH1:H2 circuits, initial rates of 0.1, 0.02 and 0.01/min were observed during the first 10 min of catalysis in the presence of 5, 1 and 0.5 nM pure C1, respectively. The cotranscribed H1:H2 and mH1:H2 circuits that were triggered by cotranscription of 1 ng of C1 also demonstrated comparable initial catalytic rates of 0.01/min (background-subtracted).

Amazingly, our results demonstrate that strand displacement does not appear to be hindered by having to 'leap' one or two mismatches (see Supplementary Figures S3–S5). The strategic introduction of mismatches has allowed us to cotranscriptionally synthesize RNA CHA circuits that operate with minimal non-catalyzed background duplex assembly while demonstrating highly sequence-specific catalytic response. Designed mismatch

placement may prove to be a generalizable means of decreasing noise in nucleic acid circuits.

Transcribing RNA signal transducers for nucleic acid diagnostics

Non-enzymatic nucleic acid amplification circuits have recently been adapted into novel diagnostic tools for sequence-specific detection of amplicons generated by enzymatic amplification (11). These nucleic acid devices function not only in solution but also operate on solid surfaces such as paper (33). The use of cotranscriptionally generated RNA circuits as similar transducers might further simplify the production of nucleic acid circuits for point-of-care applications; instead of producing, purifying and storing multiple kinetically trapped nucleic acid substrates, double-stranded transcription templates could generate these substrates on the fly.

However, as RNA:RNA base pairs are typically more stable than DNA:RNA base pairs, the RNA circuitry must be carefully designed to ensure that DNA amplicons can strand-invade and trigger the CHA reaction. To determine the feasibility of using RNA circuits for detecting ssDNA amplicons, we attempted to adapt RNA CHA to a well-known isothermal amplification method, SDA (Figure 5b). SDA is powered by strand displacing DNA polymerases such as the mesophilic enzyme Klenow fragment (3′→5′ exo-) and the thermophilic enzyme *Bst* 2.0. The repetitive primer extension and strand displacement is facilitated by inclusion of a nicking endonuclease such as the mesophilic enzyme Nb.BbvCI or the thermophilic enzyme Nb.BsrDI that recognizes 6–7-nt-long sites on double-stranded DNA and cleave only one of the DNA strands. The resulting 3′-OH group generated at the nicked site can then be extended by the DNA polymerase leading to displacement of the nicked ssDNA. Multiple cycles of extension and nicking allow accumulation of ssDNA amplicons. DNA CHA circuits have been previously used for the real-time sequence-specific detection of these SDA amplicons (12), and these DNA circuits were used as starting points for the design of their RNA counterparts. A template that could generate multiple ssDNA amplicons corresponding to the CHA catalyst C1 (with a 5′-[3*][2*][1*]-3′ domain architecture, see Figure 1) was used as the initial analyte for detection.

Isothermal amplification by SDA led to the accumulation of ssDNA copies of C1, which in turn could be used to trigger the cotranscribed RNA CHA circuit (Figure 5b). The accumulated SDA products (generated on 90 min of amplification in the absence or presence of 10 nM template) were denatured for 5 min at 95°C and then added to either cotranscribed unpurified H1 and H2 hairpins or to hairpins purified via Sephadex G25 size exclusion chromatography. Amplicon detection and circuit performance were monitored at 52°C using 100 nM RepF preannealed to an excess of RepQ.

Although the RNA version of C1 catalyzed hairpin assembly of cotranscribed mH1:H2 RNA CHA circuit, the SDA-generated ssDNA C1 failed to activate the RNA circuit (Supplementary Figure S7). This result suggested that the DNA catalyst might be inefficient at strand displacement. To overcome this hypothesized barrier, the DNA catalyst (C1234) was extended at its 5′-end by the addition of a second 8-bp toehold specific for the mH1 single-stranded loop (Figure 5c). The increased stability and stacking energy from two toeholds on either flank of the branch migration domains might overcome the energy barrier for displacing an RNA strand. Furthermore, on binding of the extended DNA catalyst to the first toehold in the mH1 loop, even partial exchange of the adjacent mH1 RNA stem by the DNA catalyst might expose enough domain 3* for productive interactions with H2.

To test our hypothesis, we incubated unpurified or column-purified cotranscribed mH1:H2 RNA CHA circuit with end-point SDA reaction products generated in the presence or absence of 10 nM template 1234LTRSDA whose amplification leads to accumulation of the extended ssDNA catalyst designated C1234. We observed that the SDA-generated C1234 ssDNA catalyst (with a 5′-[4][3*][2*][1*]-3′ domain architecture) was in fact capable of catalyzing the reaction of the mH1:H2 RNA CHA circuit and led to an increase in fluorescence over time (Figure 6a and Supplementary Figure S7). As expected, SDA reactions incubated without specific template failed to activate the RNA CHA circuit. Hairpin mH1 alone (which contained fluorescent reporter binding domains) yielded some signal when incubated with the SDA-generated C1234 ssDNA catalyst, but the signal was greatly increased due to catalytic amplification in the presence of cotranscribed H2. Thus, although some catalyst-specific signal was generated just due to mH1-mediated interactions with the reporter, the majority of signal was generated due to C1234-catalyzed initiation of RNA CHA.

The RNA CHA circuitry could also be used for the real-time detection of SDA. Because the optimal operating temperature of the mH1:H2 RNA CHA circuit was 52°C, the model 1234LTRSDA template described earlier in the text was further modified to include a nicking site for a thermostable endonuclease (Nb.BsrDI) (see Figure 5b for SDA schematic). The 1234HTRSDA template was used in SDA reactions along with a previously cotranscribed mH1:H2 RNA CHA circuit added directly to the SDA reactions without purification. Irrespective of the degree of purification, the RNA CHA circuit could accurately report the real-time accumulation of C1234 SDA amplification products (Figure 6b). As low as 1 nM template DNA could be readily detected in real-time (Supplementary Figure S8).

These results show that RNA CHA is a viable sequence-specific signal transducer that can be adapted for detection the end point or real-time detection of single-stranded DNA targets and amplicons. The simplicity of generating large quantities of RNA circuits via one-pot enzymatic cotranscription without purification or refolding makes RNA circuits an attractive alternative for not only diagnostic applications but also for the construction of more complex computational circuitry.

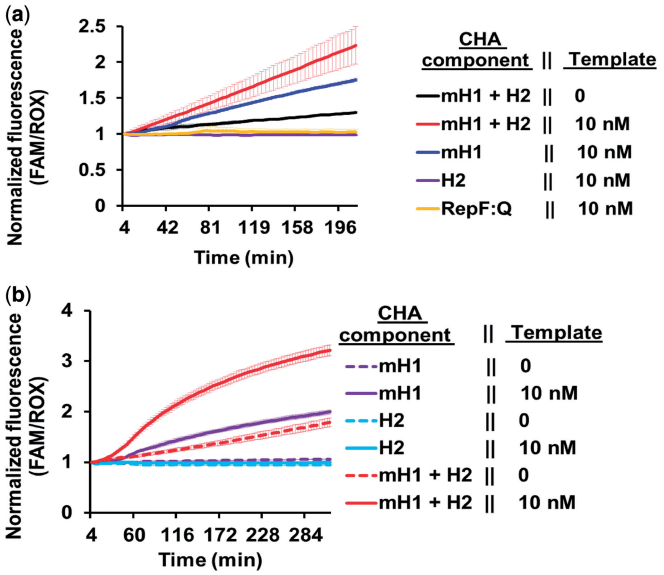

Figure 6. Cotranscriptionally generated RNA CHA as signal transducer for nucleic acid diagnostics. (**a**) End-point sequence-specific detection of SDA-generated ssDNA targets by RNA CHA. Samples with or without 10 nM template 1234LTRSDA were amplified by SDA for 90 min at 37°C in 25 µl of reaction volumes. Reactions were then incubated at 95°C for 5 min and stored at room temperature before assay by RNA CHA. Five microliters of these SDA products was then probed with 2 µl of Sephadex G25 column-purified cotranscribed mH1:H2 RNA CHA circuit. RNA CHA cotranscriptions were performed with T7 RNA polymerase using 50 ng each of the mH1 and H2 transcription templates for 1 h at 42°C. End-point RNA CHA detection reactions were assembled in 1× TNaK buffer containing 20 U of RNaseOUT, 0.5 µM ROX reference dye and 100 nM RepF (annealed with 5× excess RepQ) fluorescent DNA reporter duplex for quantitating RNA CHA in real-time at 52°C. Negative control reactions lacking RNA CHA components or containing 2 µl of either only mH1 or H2 were also tested. (**b**) Real-time signal transduction of ssDNA-generating SDA by cotranscribed mH1:H2 RNA CHA. High temperature (55°C) SDA reactions were set up with or without 10 nM 1234HTRSDA template in 20 µl of volume containing 0.5 µM ROX reference dye and 75 nM RepF (annealed with 5× excess RepQ) fluorescent DNA reporter duplex for quantitating RNA CHA in real-time. Real-time sequence-specific signal transduction was achieved by adding 2 µl of unpurified mH1:H2 RNA CHA circuits cotranscribed from 50 ng of each transcription template to the SDA reactions. Control SDA reactions containing no RNA CHA components or 2 µl of either only mH1 or H2 were also tested.

Transcriptional generation of an RNA amplifier circuit and a fluorescent RNA reporter

Our results demonstrated that cotranscriptionally generated RNA circuits could execute with minimal background. We have also adapted RNA CHA to function as a reporter for isothermal amplification reactions. These adaptations of RNA CHA have required that oligonucleotides bearing a fluor and quencher pair be added to the reaction. To further simplify the transduction scheme, we sought to use a 'label-free' fluorescent RNA signal transducer that could be generated by transcription alone for quantitation of RNA CHA reactions. An RNA aptamer (Spinach) has been reported that binds to the fluorophore DFHBI [(Z)-4-(3,5-difluoro-4-hydroxybenzylidene)-1,2-dimethyl-1H-imidazol-5(4H)-one], leading to a large increase in its fluorescence emission (34). Therefore, we engineered Spinach into a sequence-dependent fluorescent aptamer beacon (Spinach.ST) that remains conformationally trapped into an inactive state unable to bind DFHBI until it interacts with a specific sequence target (Figure 7).

To enable the application of Spinach.ST aptamer beacons in our CHA, a new CHA fuel H1B was created by replacing the domain 6* of H1 with a sequence complementary to domain 6 (the basal stem) of Spinach.ST1. When present in a duplex with H2, the exposed toehold 2* of H1B will bind to the toehold domain 2 of Spinach.ST1, initiating branch migration through domain 5 and the duplicate domain 6, regenerating the Spinach basal stem and conformation allowing it to complex with the fluorophore DFHBI (Figure 7).

An entirely RNA-based CHA circuit that processes RNA input and generates fluorescent RNA output was established by separately transcribing templates for the circuit fuels H1B and H2, the catalyst C1 and the reporter Spinach.ST1. Transcripts were filtered through Sephadex G25 and incubated at 37°C in 1× TNaK buffer containing 70 µM of the fluorophore DFHBI (Figure 8a). Although Spinach.ST1 by itself demonstrated negligible fluorescence, background duplex formation by CHA fuels H1B and H2 in the absence of C1 resulted in ~1.25-fold increase in Spinach.ST1 fluorescence over ~16 h. In contrast, the C1-catalyzed CHA reaction resulted in ~2.5-fold overall increase in Spinach.ST1 fluorescence.

To directly compare the efficiency of Spinach.ST1 with the DNA FRET reporter duplex H1BF:H1BQ, the RNA CHA circuit was assembled from gel-purified (rather than size exclusion-purified) RNA components. Some 1 µM of purified H1B and H2-fueled CHA reactions were assembled in which the amount of C1 was titrated from 0 to 100 nM. Spinach.ST1 (+ 70 µM DFHBI) or H1BF (annealed with 2× concentration of H1BQ) was included at 1 µM concentrations to monitor CHA execution. The H1BF:H1BQ DNA FRET reporter clearly outperformed the Spinach.ST1 aptamer beacon and yielded better signal-to-noise ratios at all tested concentrations of the catalyst (Figure 8b–d). Better relative performance of H1BF:H1BQ might be partly due to the 4-fold greater brightness of FAM compared with DFHBI in Spinach [http://www.glenresearch.com/Technical/Extinctions.html; (34)] or because the displacement rate of H1BQ from the H1BF:H1BQ duplex might be faster than the rate of refolding of the Spinach aptamer. Although Spinach.ST is a less efficient reporter than the DNA FRET reporter duplex previously used, the fact that it can be transcribed in a manner similar to the other components of the system opens the way to the design and execution of more complex circuits both *in vitro* and *in vivo*.

Computations with transcriptionally generated RNA circuits and reporters

Our results provide an interesting proof-of-principle demonstration for a fully RNA I/O CHA circuit that can be transcribed to process RNA inputs and generate readable RNA outputs. To further show the potential of such

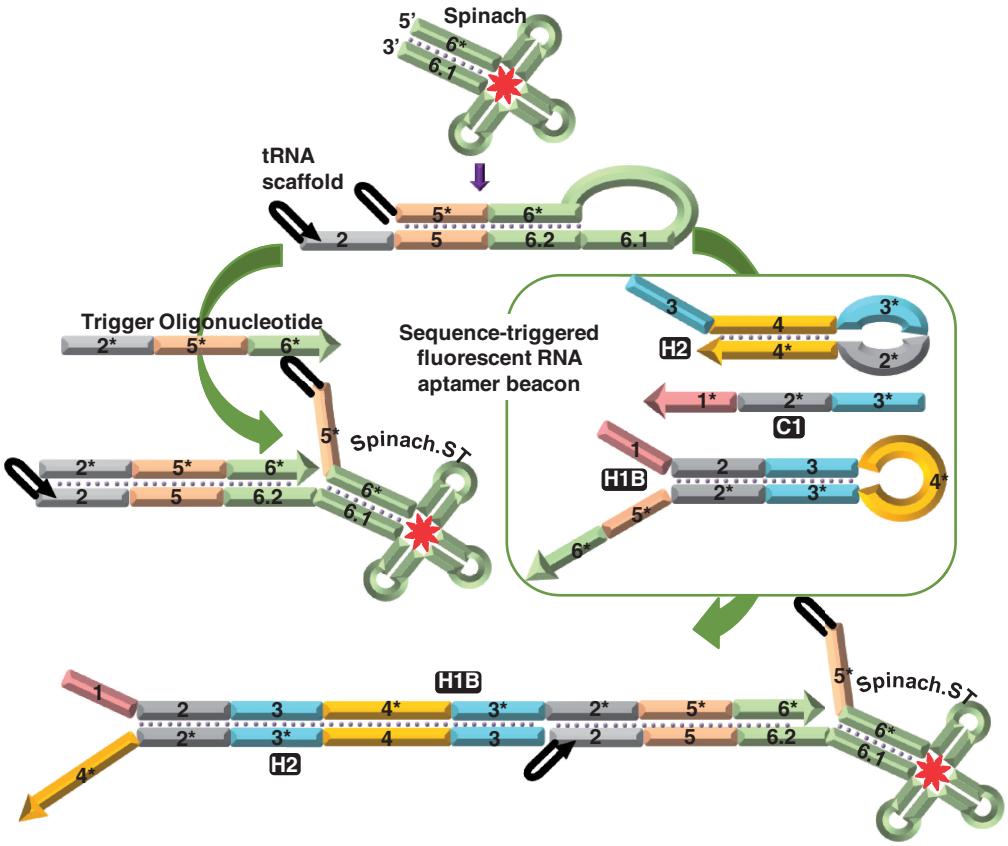

Figure 7. Reengineering of the fluorophore-dependent fluorescent RNA aptamer Spinach into sequence-triggered aptamer beacons (Spinach.ST). The fluorophore DFHBI bound to Spinach.ST1 is indicated as a red stellate. Spinach.ST is embedded within a transfer RNA scaffold and is therefore not subjected to RNA end processing by hammerhead ribozymes.

circuitry, we attempted a simple computational task, the determination of an OR Boolean logic function (Figure 9). A second RNA catalyst (C2) was designed for the hairpin H1B that could be released from its kinetic trap by either input catalyst RNA C1 or C2. Although C1 uses H1B domain 1 as the toehold to initiate strand displacement through the entire H1B stem, C2 uses a part of the H1B loop domain 4* as a toehold to displace only domain 3* of the H1B stem. The newly opened 3* domain of H1B can then function as a toehold for hybridization with H2, leading to complete displacement of the C2 catalyst.

Circuit components (H1B and H2 RNA hairpins), reporter RNA (Spinach.ST1) and the inputs C1 and C2 were separately transcribed *in vitro* and purified by filtration through Sephadex G25. These components formed an OR logic processor that operated in 1× TNaK buffer containing 70 μM DFHBI. The RNA CHA circuit was found to readily report the presence of either catalyst C1 or C2 (Figure 9b), although the initial catalytic rate with C2 was observed to be faster than the initial rate with C1 (Supplementary Figure S9). This difference may be due to the fact that C2 is completely displaced by the interactions between H1 and H2, whereas C1 can still bind over a short region (interactions between domain 1 and 1*). It is also possible that the faster initial rate with C2 could be due to quicker transcription (as it is shorter than C1) and the lack of processing (C2 lacks ribozyme flanks). Additionally, Spinach.ST1 activated by H1:H2:C1 duplexes containing C1 bound through domain 1 interactions might generate a slightly lower fluorescent signal, as it has been observed that increasing length of the aptamer basal stem tends to decrease aptamer fluorescence (J. W. Ellefson, personal communication). C2 being completely displaced from H1 on H2 binding would not yield H1:H2:C2 complexes. It was impressive that both catalysts in fact worked in a sequence-specific manner despite these differences in design, size and processing. When the circuit was presented with a 1:1 mixture of C1 and C2 in the same input volume as used with C1 or C2 alone, it was activated to almost similar levels as with C2 alone.

CONCLUSIONS

Our results firmly establish RNA as an alternate information processing and signaling molecule for engineering nucleic acid devices and automata. Structural free energy (ΔG) proved to be a reliable metric for predicting circuit kinetics, and the RNA circuit reported in this article demonstrated similar kinetics of operation when compared with the original DNA circuit from which it is

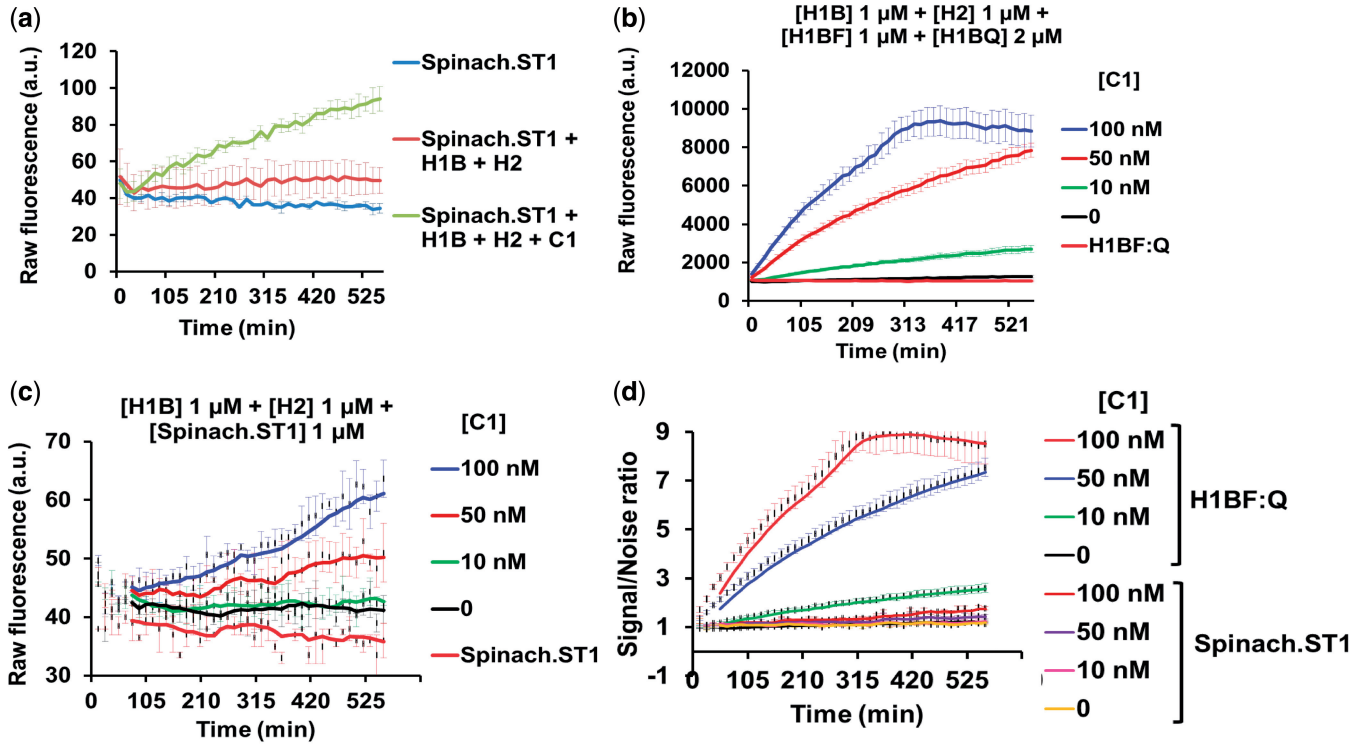

Figure 8. An entirely RNA-based CHA circuit operation and fluorimetric detection. (**a**) CHA circuit components (hairpins H1B and H2 and catalyst C1) and the RNA reporter Spinach.ST1 were separately transcribed by T7 RNA polymerase from 500 ng of PCR-generated duplex DNA transcription templates. H1B, H2 and C1 transcription templates were amplified using primers complementary to the exact ends of the cloned inserts (H1B.amp.F:H1B.amp.R, H2.amp.F:H2.amp.R and C1.amp.F:C1.amp.R, respectively) rather than the flanking plasmid. Spinach.ST transcription templates were amplified using primers specific to the flanking plasmid sequence at the 5′-end (pCR2.1.F) and the primer sphT.U.R specific to the 3′-end sequence of Spinach.ST. Transcription reactions were filtered through Sephadex G25 columns before circuit assembly. Three microliters of H1B, H2, C1 and Spinach.ST1 transcripts was mixed in indicated combinations and incubated in 1× TNaK buffer containing 70 μM DFHBI and 20 U of RNaseOUT. Circuit output was measured as increasing fluorescence intensity over time at 37°C. (**b–d**) Performance of DNA reporter duplex H1BF:H1BQ (b) versus Spinach.ST1 (c) in measuring RNA CHA circuit output. Indicated concentrations of gel-purified RNA hairpins H1B and H2 were incubated with equal concentration of H1BF:H1BQ or gel-purified Spinach.ST1 (+ 70 μM DFHBI) in the presence of titrating concentrations of pure C1 RNA. All circuits were operated in 1× TNaK buffer containing 20 U of RNaseOUT at 37°C, and average data from triplicate experiments are represented. Signal-to-noise ratio of H1BF:H1BQ versus Spinach.ST1 over the time course of RNA CHA detection is plotted in (d).

derived. This demonstration paves the way to circuits that can be entirely generated by transcription.

The conceptual demonstration was underpinned by a number of important technical demonstrations. We show that using ribozyme-mediated end processing of transcripts can easily generate substrates for RNA circuits without requiring further downstream purification and/or refolding of each individual circuit component. Enzymatic synthesis potentially provides much greater fidelity compared with chemical synthesis but at a lower cost (35,36). Chemically synthesized oligonucleotides usually demonstrate deletions at a rate of 1 in 100 bases and mismatches and insertions at ~1 in 400 bases, whereas the T7 RNA polymerase is reported to have a nucleotide substitution error rate of $<6 \times 10^{-5}$ and a deletion error rate of 6×10^{-5} (36,37). Such differences have proven to be surprisingly important for DNA circuits, where enzymatically synthesized material routinely outperforms chemically synthesized material, in part because it allows more uniform folding of the kinetically trapped substrates (24,38).

There will be additional challenges along the way to generating one-pot nucleic acid circuits based solely on cotranscription of templates. For the present study, we chose to separate circuit transcription from its application in real-time detection of DNA, as the varied reactions such as transcription, cotranscriptional ribozyme-mediated RNA circuit processing, isothermal nucleic acid amplification and circuit execution have been optimized for differing buffers and temperatures (e.g. many isothermal amplification reactions occur in excess of 65°C, whereas transcription with T7 RNA polymerase proceeds at a maximum of 42°C). Improved sequence design, reagent choices and multiplex optimizations should eventually result in the identification of substrates, enzymes and reaction conditions where all of the partners work harmoniously.

RNA circuits may prove to have a variety of applications. Recently, non-enzymatic nucleic acid amplification circuits have been used as sequence-specific signal transducers of enzymatic isothermal amplification reactions in solution and also on solid platforms such as paper fluidics aimed for point-of-care devices (11,33). Conformational stability and long-term storage of nucleic acid circuits is a critical issue for successful translation into diagnostics. The ability to cotranscriptionally generate nucleic acid circuits opens the possibility of long-term circuit storage in the form of double-stranded transcription templates

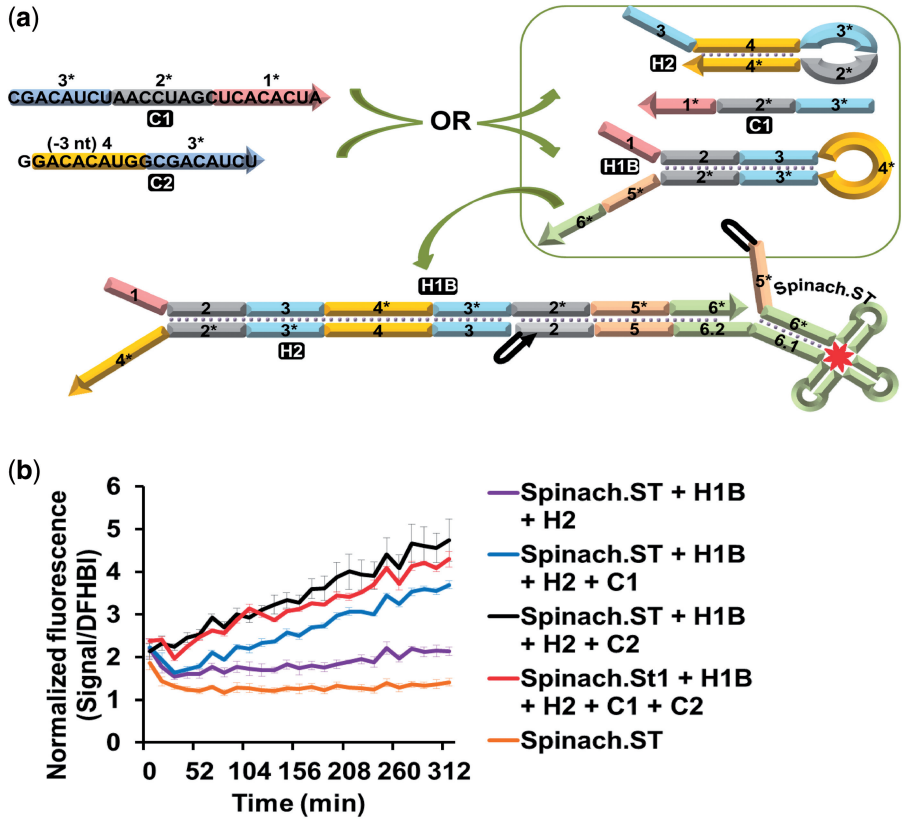

Figure 9. Application of RNA CHA circuit as an OR logic processor. (**a**) Schematic of RNA CHA circuit operation in response to either catalyst C1 OR C2. The RNA hairpin H1B serves as the OR gate, and circuit output is measured fluorimetrically using Spinach.ST1 RNA aptamer beacon. (**b**) Circuit components (H1B and H2 RNA hairpins), reporter RNA (Spinach.ST1) and the inputs C1 and C2 were transcribed from 500 ng of duplex DNA transcription templates using T7 RNA polymerase. Transcription templates were prepared using the same procedure as Figure 8. Following filtration through Sephadex G25, 3 µl/transcript (or 1.5 µl each of C1 and C2 when added together in a reaction) was mixed in the indicated combinations in 1× TNaK buffer containing 70 µM DFHBI and 20 U of RNaseOUT. Circuits were operated at 37°C, and outputs were measured fluorimetrically.

from which circuits could be synthesized in real-time or as needed during diagnostic application.

Finally, RNA is an especially attractive medium for executing nucleic acid circuits *in vivo* because it might fold during transcription into engineered conformations amenable to computation and regulation. Thus, the formulation of design principles for RNA circuits should eventually translate into a toolbox for synthesis and operation of complex non-enzymatic nucleic acid circuits *in vivo* (8,9). Because hammerhead ribozymes have been extensively used for *in vivo* RNA processing (39,40), *in vitro* validation of ribozyme-mediated cotranscriptional generation of RNA circuit components opens the way for *in vivo* implementation of similar expression strategies. In fact, coregulated expression of circuit components could be achieved by constructing expression cassettes containing a series of circuit components with intervening ribozymes for cleavage into individual units. It has been noted previously that the transcription start site of riboregulators has a dramatic effect on their *in vivo* activity (9). By removing unwanted header sequences from transcripts using ribozyme-mediated RNA processing, such variation might be readily minimized. Replacement of the minimal hammerhead ribozyme sequences used here for *in vitro* processing with hammerhead ribozyme sequences selected for *in vivo* activity might improve the yield of active circuit components (41). Another important outcome of the current work was the conceptualization and demonstration of strategically placed mismatches within the circuit as a means of preventing unwanted interaction between circuit components leading to higher background noise during co-transcription. Although it is possible to temporally regulate *in vivo* expression of circuit components to prevent unintended interactions, especially during RNA synthesis, the use of mismatches may be a more elegant, simpler and enabling solution to cotranscriptional *in vivo* circuit synthesis and execution. Furthermore, sequence-dependent Spinach RNA aptamer beacon engineered during this work can potentially enable direct *in vivo* visualization of RNA conformational changes and assembly instead of relying on the indirect translational fluorescent protein reporters.

SUPPLEMENTARY DATA

Supplementary Data are available at NAR Online.

ACKNOWLEDGEMENTS

The authors would like to thank Dr Xi Chen for helpful discussions.

FUNDING

Welch Foundation [F1654]; Department of Defense National Security Science and Engineering Faculty Fellowship [FA9550-10-1-0169]; and National Institutes of Health EUREKA [5 R01 GM094933-01,02,03]. Funding for open access charge: National Institutes of Health EUREKA [5 R01 GM094933-01,02,03].

Conflict of interest statement. None declared.

REFERENCES

1. Chen,X. and Ellington,A.D. (2010) Shaping up nucleic acid computation. *Curr. Opin. Biotechnol.*, **21**, 392–400.
2. Li,B., Ellington,A.D. and Chen,X. (2011) Rational, modular adaptation of enzyme-free DNA circuits to multiple detection methods. *Nucleic Acids Res.*, **39**, e110.
3. Qian,L., Winfree,E. and Bruck,J. (2011) Neural network computation with DNA strand displacement cascades. *Nature*, **475**, 368–372.
4. Zhang,D.Y. and Seelig,G. (2011) Dynamic DNA nanotechnology using strand-displacement reactions. *Nat. Chem.*, **3**, 103–113.
5. Qian,L. and Winfree,E. (2011) Scaling up digital circuit computation with DNA strand displacement cascades. *Science*, **332**, 1196–1201.
6. Seelig,G., Soloveichik,D., Zhang,D.Y. and Winfree,E. (2006) Enzyme-free nucleic acid logic circuits. *Science*, **314**, 1585–1588.
7. Choi,H.M., Chang,J.Y., Trinh le,A., Padilla,J.E., Fraser,S.E. and Pierce,N.A. (2010) Programmable in situ amplification for multiplexed imaging of mRNA expression. *Nat. Biotechnol.*, **28**, 1208–1212.
8. Lucks,J.B., Qi,L., Mutalik,V.K., Wang,D. and Arkin,A.P. (2011) Versatile RNA-sensing transcriptional regulators for engineering genetic networks. *Proc. Natl Acad. Sci. USA*, **108**, 8617–8622.
9. Isaacs,F.J., Dwyer,D.J., Ding,C.M., Pervouchine,D.D., Cantor,C.R. and Collins,J.J. (2004) Engineered riboregulators enable post-transcriptional control of gene expression. *Nat Biotechnol*, **22**, 841–847.
10. Yin,P., Choi,H.M., Calvert,C.R. and Pierce,N.A. (2008) Programming biomolecular self-assembly pathways. *Nature*, **451**, 318–322.
11. Li,B., Chen,X. and Ellington,A.D. (2012) Adapting enzyme-free DNA circuits to the detection of loop-mediated isothermal amplification reactions. *Anal. Chem.*, **84**, 8371–8377.
12. Jiang,Y.S., Li,B., Milligan,J.N., Bhadra,S. and Ellington,A.D. (2013) Real-time detection of isothermal amplification reactions with thermostable catalytic hairpin assembly. *J. Am. Chem. Soc.*, **135**, 7430–7433.
13. Zadeh,J.N., Steenberg,C.D., Bois,J.S., Wolfe,B.R., Pierce,M.B., Khan,A.R., Dirks,R.M. and Pierce,N.A. (2011) NUPACK: analysis and design of nucleic acid systems. *J. Comput. Chem.*, **32**, 170–173.
14. Dirks,R.M., Bois,J.S., Schaeffer,J.M., Winfree,E. and Pierce,N.A. (2007) Thermodynamic analysis of interacting nucleic acid strands. *SIAM Rev.*, **49**, 65–88.
15. Dirks,R.M. and Pierce,N.A. (2003) A partition function algorithm for nucleic acid secondary structure including pseudoknots. *J. Comput. Chem.*, **24**, 1664–1677.
16. Dirks,R.M. and Pierce,N.A. (2004) An algorithm for computing nucleic acid base-pairing probabilities including pseudoknots. *J. Comput. Chem.*, **25**, 1295–1304.
17. Kim,J. and Winfree,E. (2011) Synthetic *in vitro* transcriptional oscillators. *Mol. Syst. Biol.*, **7**, 465.
18. Franco,E., Friedrichs,E., Kim,J., Jungmann,R., Murray,R., Winfree,E. and Simmel,F.C. (2011) Timing molecular motion and production with a synthetic transcriptional clock. *Proc. Natl Acad. Sci. USA*, **108**, E784–E793.
19. Simpson,Z.B., Tsai,T.L., Nguyen,N., Chen,X. and Ellington,A.D. (2009) Modelling amorphous computations with transcription networks. *J.R. Soc. Interface*, **6(Suppl. 4)**, S523–S533.
20. Kim,J., White,K.S. and Winfree,E. (2006) Construction of an *in vitro* bistable circuit from synthetic transcriptional switches. *Mol. Syst. Biol.*, **2**, 68.
21. Hockenberry,A.J. and Jewett,M.C. (2012) Synthetic *in vitro* circuits. *Curr. Opin. Chem. Biol.*, **16**, 253–259.
22. Delebecque,C.J., Lindner,A.B., Silver,P.A. and Aldaye,F.A. (2011) Organization of intracellular reactions with rationally designed RNA assemblies. *Science*, **333**, 470–474.
23. Lesnik,E.A. and Freier,S.M. (1995) Relative thermodynamic stability of DNA, RNA, and DNA:RNA hybrid duplexes: relationship with base composition and structure. *Biochemistry*, **34**, 10807–10815.
24. Chen,X., Briggs,N., McLain,J.R. and Ellington,A.D. (2013) Stacking nonenzymatic circuits for high signal gain. *Proc. Natl Acad. Sci. USA*, **110**, 5386–5391.
25. Milligan,J.F., Groebe,D.R., Witherell,G.W. and Uhlenbeck,O.C. (1987) Oligoribonucleotide synthesis using T7 RNA polymerase and synthetic DNA templates. *Nucleic Acids Res.*, **15**, 8783–8798.
26. Rosa,M.D. (1979) Four T7 RNA polymerase promoters contain an identical 23 bp sequence. *Cell*, **16**, 815–825.
27. Krupp,G. (1988) RNA synthesis: strategies for the use of bacteriophage RNA polymerases. *Gene*, **72**, 75–89.
28. Price,S.R., Ito,N., Oubridge,C., Avis,J.M. and Nagai,K. (1995) Crystallization of RNA-protein complexes. I. Methods for the large-scale preparation of RNA suitable for crystallographic studies. *J. Mol. Biol.*, **249**, 398–408.
29. Ke,A. and Doudna,J.A. (2004) Crystallization of RNA and RNA-protein complexes. *Methods*, **34**, 408–414.
30. Martin,C.T., Muller,D.K. and Coleman,J.E. (1988) Processivity in early stages of transcription by T7 RNA polymerase. *Biochemistry*, **27**, 3966–3974.
31. Zhang,D.Y. and Winfree,E. (2009) Control of DNA strand displacement kinetics using toehold exchange. *J. Am. Chem. Soc.*, **131**, 17303–17314.
32. Meyer,I.M. and Miklos,I. (2004) Co-transcriptional folding is encoded within RNA genes. *BMC Mol. Biol.*, **5**, 10.
33. Allen,P.B., Arshad,S.A., Li,B., Chen,X. and Ellington,A.D. (2012) DNA circuits as amplifiers for the detection of nucleic acids on a paperfluidic platform. *Lab Chip*, **12**, 2951–2958.
34. Paige,J.S., Wu,K.Y. and Jaffrey,S.R. (2011) RNA mimics of green fluorescent protein. *Science*, **333**, 642–646.
35. Hecker,K.H. and Rill,R.L. (1998) Error analysis of chemically synthesized polynucleotides. *Biotechniques*, **24**, 256–260.
36. Tian,J.D., Gong,H., Sheng,N.J., Zhou,X.C., Gulari,E., Gao,X.L. and Church,G. (2004) Accurate multiplex gene synthesis from programmable DNA microchips. *Nature*, **432**, 1050–1054.
37. Brakmann,S. and Grzeszik,S. (2001) An error-prone T7 RNA polymerase mutant generated by directed evolution. *Chembiochem*, **2**, 212–219.
38. Zhang,D.Y. and Winfree,E. (2010) Robustness and modularity properties of a non-covalent DNA catalytic reaction. *Nucleic Acids Res.*, **38**, 4182–4197.
39. Lacadie,S.A., Tardiff,D.F., Kadener,S. and Rosbash,M. (2006) *In vivo* commitment to yeast cotranscriptiona splicing is sensitive to transcription elongation mutants. *Genes Dev.*, **20**, 2055–2066.
40. Gromak,N., Talotti,G., Proudfoot,N.J. and Pagani,F. (2008) Modulating alternative splicing by cotranscriptional. *RNA*, **14**, 359–366.
41. Chen,X., Denison,L., Levy,M. and Ellington,A.D. (2009) Direct selection for ribozyme cleavage activity in cells. *RNA*, **15**, 2035–2045.